Special Topics on Precision Measurement in Atomic Physics: Lecture 11

Forbidden Transitions

Instructor: Gordon W.F. Drake, University of Windsor
Sponsored by USTC, Organized by WIPM
October 9 to November 13, 2019

1 Forbidden Transitions

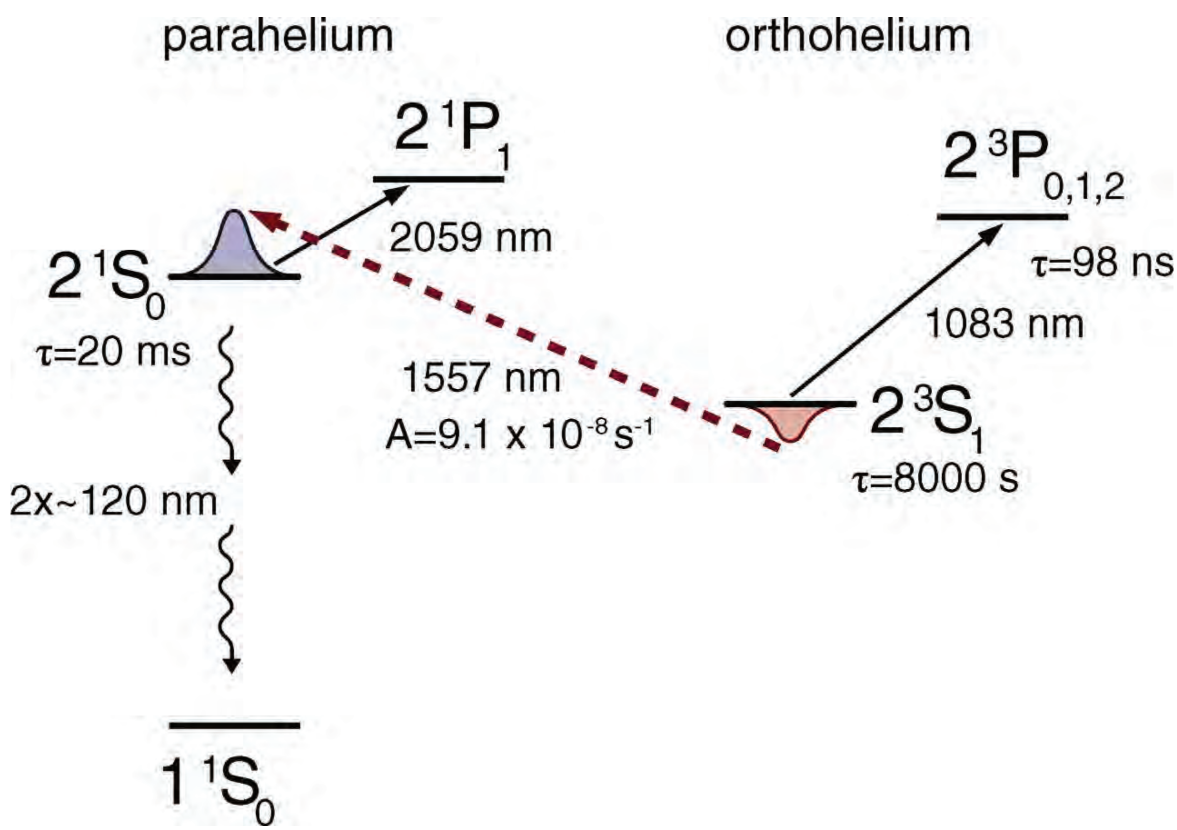

R. van Rooij, J. S. Borbely, J. Simonet, M. D. Hoogerland, K. S. E. Eikema, R. A. Rozendaal, W. Vassen Science 333, 6039 (2011)

SELECTION RULES:

- Electric dipole (E1), In LS coupling:
  - $\Delta L = 0$ or ± 1, but $L = 0 \not\to L = 0$
  - $\Delta S = 0$
  - $\Delta J = 0$ or ± 1, but $J = 0 \not\to J = 0$
  - Parity $\mathcal{P}$ is odd
- Magnetic dipole (M1):
  - $\Delta L = 0$ or ± 1,
  - $\Delta S = 0$ or ± 1
  - $\Delta J = 0$ or ± 1, but $J = 0 \not\to J = 0$
  - Parity $\mathcal{P}$ is even

ORDERS OF MAGNITUDE

For the Einstein A-coefficient (per unit time)

- E1: $A \sim (\omega/c)^3 \langle r \rangle^2 \sim \alpha^3 Z^6 Z^{-2} = \alpha^3 Z^4$ if $\Delta n \neq 0$ $(\sim 10^9\ \mathrm{s}^{-1})$
  $= \alpha^3 Z$ if $\Delta n = 0$
- M1: $A \sim (\mathrm{E1}) \times \alpha^2 Z = \alpha^5 Z^2$ if $\Delta n = 0$
- Relativistic M1: $A \sim (\mathrm{E1}) \times (\alpha^2 Z^2)(\alpha^2 Z^2)^2 = \alpha^9 Z^{10}$ $(\sim 10^{-4}\ \mathrm{s}^{-1}$ for He)
- M2: $A \sim (\mathrm{E1}) \times (\alpha^2 Z^2)^2 = \alpha^7 Z^8$ (Exceeds E1 at $Z \sim 18$ if $\Delta n = 0$)
- spin-forbidden E1: $A \sim (\mathrm{E1}) \times \left(\dfrac{\alpha^2 Z^4}{Z}\right)^2 = \alpha^7 Z^{10}$

Note that for the transition energy, $\hbar\omega \propto \begin{cases} Z^2, & \Delta n \neq 0, \\ Z, & \Delta n = 0 \end{cases}$

RADIATIVE TRANSITIONS IN ONE– AND TWO–ELECTRON IONS

Gordon W. F. Drake and A. van Wijngaarden

Department of Physics
University of Windsor
Windsor, Ontario N9B 3P4, Canada

INTRODUCTION

This series of lectures has a rather general title because it deals with a variety of topics, both theoretical and experimental, which are related to one another. A great deal of progress has been made over the past few years in the precision of measurements for one– and two–electron atoms. A parallel development of new techniques for high precision caculations is opening the way to a wide variety of comparisons between theory and experiment which are sensitive to higher order relativistic and quantum electrodynamic (QED) effects. There are close connections between these lectures, which focus primarily on the low to intermediate range of nuclear charge, and those of Peter Mohr and Berndt Müller, which describe effects in the high nuclear charge and super–critical field regimes.

The first lecture will begin with a review of the basic theory of radiative transitions in order to define the notation and lay the ground work for a discussion of the interference effects which occur in the electric field quenching of hydrogenic ions. I will then describe in some detail the quenching anisotropy method for measuring the Lamb shift, which has recently yielded the most accurate available determination of the Lamb shift in He^+, thereby providing one of the most sensitive tests of higher order QED corrections.

The second lecture will begin with a brief description of closely related quenching asymmetry measurements which yield the level width of the 2p state, and the relativistic magnetic dipole matrix element for the $2\ ^2S_{1/2} - 1\ ^2S_{1/2}$ transition. I will then change topics to a discussion of new variational techniques for two–electron atoms. These techniques now make it possible to improve the precision of existing calculations by several orders of magnitude for nonrelativistic energies and relativistic corrections of $O(\alpha^2)$. This improvement is necessary in order to match the accuracy of existing measurements. An important advantage of these techniques is that they can be extended to higher members of the Rydberg series (at least up to $n \sim 10$) with no serious loss of accuracy. In contrast, standard variational calculations suffer a disasterous loss of accuracy for the more highly excited states.

The third lecture will begin with a summary of the numerous small corrections to the two–electron energy which must be included before a comparison with experiment becomes meaningful. These are finite nuclear mass effects of $O(\mu/M)$ and $O(\mu^2/M^2)$, relativistic corrections of $O(\alpha^2)$, relativistic reduced mass corrections of $O(\alpha^2\mu/M)$ and QED corrections of $O(\alpha^3Z^4)$ and higher. For the QED terms, the two–electron corrections of $O(\alpha^3Z^3)$ referred to as the "screening of the Lamb shift" are included in a nonrelativistic approximation in which the leading term is evaluated exactly, and the relativistic corrections of $O(\alpha^4Z^4)$ and higher are estimated from the corresponding one–electron terms. An exact calculation of the two–electron relativistic corrections has not yet been done, although progress on this topic is reviewed in Peter Mohr's talk. A comparison with a wide variety of high precision transition frequency measurements yields well–defined discrepancies which can reasonably be accounted for by uncalculated terms of $O(\alpha^4Z^4)$ and $O(\alpha^3Z^2)$. Finally, a brief survey will be given of the comparison between theory and experiment for high–Z two–electron ions.

RADIATIVE TRANSITIONS

This section begins with an overview of the decay mechanisms for the low–lying states of one– and two–electron ions. Then the theory of spontaneous transitions is briefly reviewed. This establishes the basic concepts and notation for a more detailed discussion of relativistic magnetic dipole transitions and the quenching radiation asymmetries which allow one to measure the Lamb shift in one–electron ions.

Fig. 1 shows the low–lying states of one–electron ions together with their modes of radiative decay. As is well known, the $2s_{1/2}$ state is metastable because ordinary electric dipole (E1) transitions to the ground state are forbidden by the parity selection rule. For low Z ions, the dominant decay mechanisn is the simultaneous emission of two E1 photons, giving a decay rate of

$$w(2\mathrm{E1}) = 8.2293810 Z^6\ \mathrm{s}^{-1} + \text{relativistic corrections} \tag{1}$$

(Drake, 1986). However, the relativistic M1 mechanism discussed below increases in proportion to Z^{10} and eventually becomes dominant for $Z \geq 43$.

In the presence of an external electric field, the $2s_{1/2}$ state becomes mixed with the close–lying $2p_{1/2}$ and $2p_{3/2}$ states, making possible E1 and M2 transitions to the

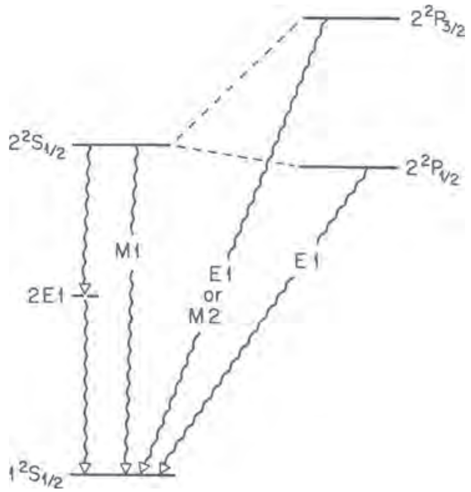

Fig. 1. Energy level diagram for one–electron ions, showing the radiative decay modes. The dashed lines indicate electric field mixing of the $2s_{1/2}$ state with the $2p_{1/2}$ and $2p_{3/2}$ states, leading to field–induced E1 (electric dipole) and M2 (magnetic quadupole) transitions to the ground state.

ground state. The external field mixing is represented by dashed lines in Fig. 1. The rotational asymmetries discussed below arise from interference effects among the single photon decay channels.

Fig. 2 is a similar diagram of the radiative decay modes for two–electron ions. Here, both the states 1s2s $^1S_0$ and 1s2s $^3S_1$ are metastable. Calculations for the 2E1 decay mode from the 2 $^1S_0$ state have recently been done to improved precision by Drake (1986), and the decay rate has been measured in ions up to Kr^{34+} (Marrus, 1986). The relativistic M1 decay rate from the 2 $^3S_1$ state was first calculated by Drake (1971, 1972a), Beigman and Safranova (1971), and by Feinberg and Sucher (1971). These processes are of considerable astrophysical importance (see, for example, Drake and Robbins, 1972; Blumenthal *et al.* 1972).

As in the one–electron case, the 2 $^1S_0$ state of helium can be quenched by the application of an electric field due to field–induced mixing with the 2 $^1P_1$ state. However, fields on the order of 100 kV/cm are required because of the large electrostatic splitting between the states. The quench rate has been measured by Petrasso and Ramsey (1972). Their result of $0.926(20)F^2(\mathrm{cm/kV})^2\mathrm{s}^{-1}$ (F is the field strength) agrees with the theoretical value $0.932(1)F^2(\mathrm{cm/kV})^2\mathrm{s}^{-1}$ obtained by Drake (1972b).

The wavy dashed lines in Fig. 2 indicate more exotic decay modes which become increasingly important for the two–electron ions of higher Z. The 2 $^3P_1$ – 1 $^1S_0$ E1 transition is a spin–forbidden process which accurs through mixing between the 2 $^1P_1$ and n $^3P_1$ states due to the Breit interaction (Drake and Dalgarno, 1969; Drake, 1976). There is also a small contribution from doubly excited npn'p $^3P_0^e$ intermediate states (Drake, 1976). The M2 decay rate from the 2 $^3P_2$ state is discussed by Drake (1969). Since it increases in proportion to Z^8 along the isoelectronic sequence, while the competing 2 $^3P_2$ – 2 $^3S_1$ E1 rate only increases as Z, the M2 process becomes dominant for ions beyond Cl^{15+}.

The very unusual E1M1 two–photon decay mode from the 2 $^3P_0$ state is discussed by Drake (1985). Even though it is strongly suppressed, the rate increases in pro–

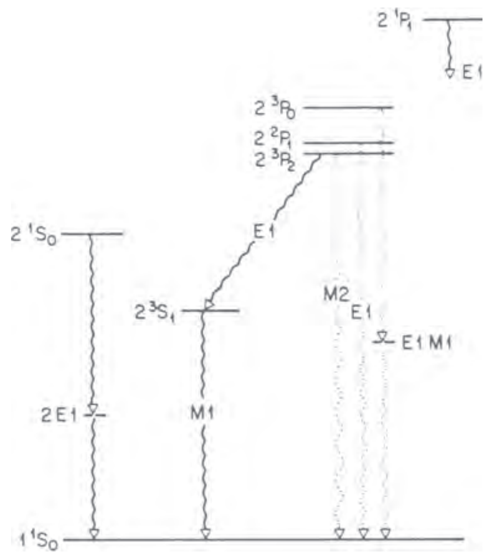

Fig. 2. Energy level diagram for two–electron ions, showing the radiative decay modes for the low–lying states. The wavy dashed lines indicate inhibited transitions which become important for high–Z ions.

portion to Z^{12}, reaching about 46% of the allowed E1 rate in U^{90+}. The Munger and Gould (1986) measurement of the $2\,^3S_1 - 2\,^3P_2$ energy splitting in U^{90+} relies on the theoretical value for the E1M1 decay rate.

Theory of Spontaneous Transitions

Fig. 3 shows the basic Feynman diagram for the spontaneous emission of a single photon. The corresponding transition rate is given by Fermi's Golden Rule

$$w = \frac{2\pi}{\hbar}|\langle f|V_{\text{int}}|i\rangle|^2\rho_{\text{f}} \tag{2}$$

where

V_{int} = interaction energy operator

ρ_{f} = no. of final states per unit energy interval.

The basic parameters which characterize the emitted photon are

ω = photon frequency

$\hat{\text{e}}$ = photon polarization vector

$\vec{\text{k}}$ = photon propagation vector ($|\vec{\text{k}}| = \omega/c$).

Then

$$\rho_{\text{f}} = \frac{\mathcal{V}k^2 d\Omega}{(2\pi)^3\hbar c} \tag{3}$$

is the number of photon states of polarization $\hat{\text{e}}$ per unit energy and solid angle in normalization volume $\mathcal{V}$. The interaction energy operator is

$$\text{V}_{\text{int}} = e\vec{\alpha}\cdot\vec{\text{A}}^* \quad . \tag{4}$$

If the photon vector potential $\vec{\text{A}}$ is normalized to a field energy of $\hbar\omega$ per unit volume, then

$$\vec{\text{A}} = \frac{1}{k}\left[\frac{2\pi\hbar\omega}{\mathcal{V}}\right]^{1/2}\hat{\text{e}}e^{i\vec{\text{k}}\cdot\vec{\text{r}}} \quad . \tag{5}$$

Collecting terms, eq. (2) becomes

$$w d\Omega = \left[\frac{e^2 k}{2\pi\hbar}\right]|\langle f|\vec{\alpha}\cdot\hat{\text{e}}e^{-i\vec{\text{k}}\cdot\vec{\text{r}}}|i\rangle|^2 d\Omega \ \text{ per unit time.} \tag{6}$$

In the nonrelativistic limit, $\vec{\alpha} \to \vec{p}/mc$, $e^{-i\vec{\text{k}}\cdot\vec{\text{r}}} \simeq 1$ and the above becomes the familiar dipole velocity form of the transition rate.

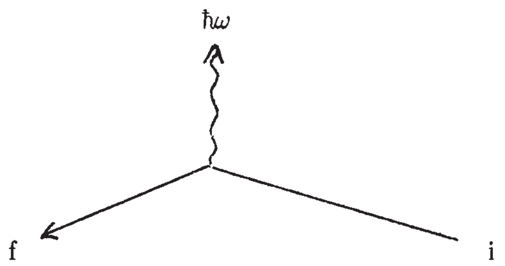

Fig. 3. Feynman diagram showing the basic lowest order process of spontaneous photon emission.

For the $2s_{1/2}$ state, E1 and M2 processes become allowed due to electric field mixing with the $2p_{1/2}$ and $2p_{3/2}$ states. A systematic way of incorporating all higher multipole moments is to use the standard multipole expansion

$$\hat{e}e^{-i\vec{k}\cdot\vec{r}} = \left[\frac{3}{8\pi}\right]^{1/2}\sum_{M} \{e_M\, \vec{a}^{(1)*}_{1,M} + i[\hat{k}\times\hat{e}]_M\, \vec{a}^{(0)*}_{1,M}$$
$$+ i\sqrt{10/3}\ [\hat{k},\, \hat{k}\times\hat{e}]_{2,M}\, \vec{a}^{(0)*}_{2,M} + \cdots \} \tag{7}$$

where

$$e_{\pm1} = \mp\frac{1}{\sqrt{2}}\,(e_x \pm ie_y), \qquad e_0 = e_z$$

and $[a,\, b]_{2,M}$ denotes the vector coupled product

$$[a,\, b]_{2,M} = \sum_{m_1,m_2} \langle 11m_1m_2|2M\rangle\, a_{m_1}b_{m_2}\ .$$

The $\vec{a}^{(\lambda)}_{LM}$ are multipole operators with

$\lambda = 1$ for electric multipoles
$\lambda = 0$ for magnetic multipoles.

In the transverse or Coulomb gauge, they are given by

$$\vec{a}^{(1)}_{LM} = \left[\frac{L}{2L+1}\right]^{1/2} g_{L+1}(kr)\ \vec{Y}^{M}_{LL+1}(\hat{r})$$
$$+ \left[\frac{L+1}{2L+1}\right]^{1/2} g_{L-1}(kr)\ \vec{Y}^{M}_{LL-1}(\hat{r}) \tag{8}$$

$$\vec{a}^{(0)}_{LM} = g_L(kr)\ \vec{Y}^{M}_{LL}(\hat{r}) \tag{9}$$

where the $\vec{Y}^{M}_{Jl}(\hat{r})$ are vector spherical harmonics defined by

$$\vec{Y}^{M}_{Jl}(\hat{r}) = \sum_{m,q} Y_l^{m}(\hat{r})\hat{e}_q(l\ 1\ m\ q|J\ M) \tag{10}$$

$$g_L(kr) = 4\pi i^L j_L(kr) \tag{11}$$

and

$$j_L(z) = \frac{z^L}{(2L+1)!!}\left[1 - \frac{z^2/2}{1!(2L+3)} + \frac{(z^2/2)^2}{2!(2L+3)(2L+5)} - \cdots\right] \tag{12}$$

is a spherical Bessel function. For low Z atoms, $kr = \omega r/c$ is small and one can make the long wavelength approximation in which only the leading term of eq. (12) is retained. In the nonrelativistic limit, the four component Dirac operators reduce to the equivalent nonrelativistic operators acting on two–component Pauli spinors

$$e\vec{\alpha}\cdot\vec{a}^{(1)}_{1M} \longrightarrow e\sqrt{2}\ \Phi_{1M}, \tag{13}$$

$$e\vec{\alpha}\cdot\vec{a}^{(0)}_{1M} \longrightarrow i(\nabla\Phi_{1M})\cdot\left[\frac{e\vec{L}}{mc\sqrt{2}} + \sqrt{2}\ \vec{\mu}\right] \tag{14}$$

and $$e\vec{\alpha}\cdot\vec{a}^{(0)}_{2M} \rightarrow i(\nabla\Phi_{2M})\cdot\left[\frac{e\vec{L}}{mc\sqrt{6}} + \sqrt{3/2}\ \vec{\mu}\right] \tag{15}$$

where $\Phi_{LM} = g_L(kr)\,Y_L{}^M(\hat{r})$, $\vec{L} = \vec{r}\times\vec{p}$, and $\vec{\mu} = (e\lambda\!\!\!^{-}/2)\vec{\sigma}$. Here, $\vec{\mu}$ is the magnetic moment operator and $\lambda\!\!\!^{-} = \alpha a_0$ is the Compton wavelength.

Relativistic Magnetic Dipole Transitions

For the $2s_{1/2} \rightarrow 1s_{1/2}$ transition, only the M1 term $\vec{a}^{(0)}_{1M}$ contributes, but even this term vanishes in the nonrelativistic long wavelength approximation since $i\nabla\Phi_{1M} \longrightarrow k(4\pi/3)^{1/2}\hat{e}_M$, and matrix elements are proportional to the overlap integral. However, relativistic corrections of $O(\alpha^2Z^2)$ and finite wavelength corrections of $O[(\omega r/c)^2]$ give

$$e\vec{\alpha}\cdot\vec{a}^{(0)}_{1M} \simeq -k\sqrt{8\pi/3}\,M_{1M} \tag{16}$$

where

$$M_{1M} = \mu_M\left[1 - \frac{2p^2}{3m^2c^2} - \frac{1}{6}\left[\frac{\omega r}{c}\right]^2 + \frac{Ze^2}{3mc^2r}\right] \tag{17}$$

is the effective magnetic moment transition operator acting on nonrelativistic wave functions. For the $2s_{1/2} \rightarrow 1s_{1/2}$ transition, the matrix elements are

$$\langle 1s_{1/2,1/2}|M^*_{1,0}|2s_{1/2,1/2}\rangle = -\left[\frac{8\alpha^2Z^2}{81\sqrt{2}}\right] e\lambda\!\!\!^{-} \tag{18}$$

$$\langle 1s_{1/2,-1/2}|M^*_{1,1}|2s_{1/2,1/2}\rangle = \left[\frac{8\alpha^2Z^2}{81}\right] e\lambda\!\!\!^{-}\ . \tag{19}$$

The transition rate into solid angle $d\Omega$ is then

$$wd\Omega = \left[\frac{k^3}{2\pi\hbar}\right]|M|^2\{|[\hat{k}\times\hat{e}]_0|^2 + 2|[\hat{k}\times\hat{e}]_1|^2\}d\Omega \tag{20}$$

with $M = -\left[\dfrac{8\alpha^2Z^2}{81\sqrt{2}}\right] e\lambda\!\!\!^{-}$. $\qquad$ (21)

Summing over any two linearly independent polarization vectors $\hat{e}$ perpendicular to $\hat{k}$ results in

$$\sum_{\hat{e}}|[\hat{k}\times\hat{e}]_0|^2 = \sin^2\theta \tag{22}$$

and

$$2\sum_{\hat{e}}|[\hat{k}\times\hat{e}]_1|^2 = 1 + \cos^2\theta\ . \tag{23}$$

Thus $\int d\Omega = \int\int \sin\theta d\theta d\varphi$ just gives a factor of 4π. Using the nonrelativistic value $k = \dfrac{3Z^2\alpha}{8a_0}$ yields the final decay rate

$$\begin{aligned} w(2s_{1/2} \rightarrow 1s_{1/2}) &= 4k^3|M|^2/\hbar \\ &= \left[\frac{\alpha^9Z^{10}}{972}\right]\tau^{-1} \\ &= 2.496\times10^{-6}\ s^{-1} \end{aligned} \tag{24}$$

for H. ($\tau = 2.41888\times10^{-17}$s is the atomic unit of time.) This is much less than the 2E1 decay rate for H. However, the M1 rate becomes dominant for $Z > 43$. Even for H and He^+, the M1 process produces observable interference effects in Stark quenching, as discussed in the following section.

1.1 Selection Rules

THE ASTROPHYSICAL JOURNAL, Vol. 158, December 1969

THE n^3P_2–1^1S_0 MAGNETIC-QUADRUPOLE TRANSITIONS OF THE HELIUM SEQUENCE

G. W. F. DRAKE*†
Smithsonian Astrophysical Observatory, Cambridge, Massachusetts
Received 1969 April 29; revised 1969 May 16

ABSTRACT

Accurate variational calculations are presented for the 2^3P_2–1^1S_0 magnetic-quadrupole decay rates of the heliumlike ions He I to Ne IX. It is shown that Z-expansion results for ^1P–^1S electric-dipole transitions are easily modified to obtain the Z-expansion of the corresponding ^3P–^1S magnetic-quadrupole transition. The Z-expansion parameters are presented for the n^3P_2–1^1S_0 transitions, with $n = 2(1)\ 20$.

I. INTRODUCTION

Recent far-ultraviolet and soft X-ray spectra of the Sun and solar corona containing transitions due to heliumlike ions of large nuclear charge have been reported by several investigators, including Neupert *et al.* (1967), Evans and Pounds (1968), Widing and Sandlin (1968), and Meekins *et al.* (1968). In some of these spectra, the intercombination 2^3P_1–1^1S_0 transitions are prominent.

For small values of the nuclear charge Z, the nine 2^3P_J states with $J = 0, 1, 2$ normally radiate to the 2^3S_1 states (J is the total electronic angular momentum defined by $J = L + S$). However, if $Z > 6$, the 2^3P_1 states preferentially radiate through the spin forbidden transition to the 1^1S_0 ground state (Drake and Dalgarno 1969). The 2^3P_0 state cannot undergo any single-photon transition to the ground state in the absence of nuclear spin, and its radiative lifetime is determined by the 2^3P_0–2^3S_1 transition. The 2^3P_2 state connects directly with the ground state through the magnetic-quadrupole transition (Mizushima 1964, 1966; Garstang 1967). This process dominates the 2^3P_2–2^3S_1 transition for large values of the nuclear charge, but remains slow in comparison with the 2^3P_1–1^1S_0 decay rate. Thus, it may be possible to observe the selective depopulation of the 2^3P_1 state of heliumlike ions with $Z > 6$ and to derive rates for collisionally induced transitions among the 2^3P fine-structure levels.

We present in this paper accurate variational calculations of the 2^3P_2–1^1S_0 magnetic-quadrupole decay rate for He I to Ne IX. The calculations are extended to higher values of the nuclear charge and to higher principal quantum numbers of the ^3P state by the Z-expansion method of Dalgarno and Parkinson (1967).

II. THEORY

The probability of magnetic-multipole radiation for an N-electron atom is, in atomic units,

$$A_{km}^{(0)} = \frac{2(k+1)}{k(2k+1)[(2k-1)!!]^2c^2}\left(\frac{\omega}{c}\right)^{2k+1} |\langle i|Q_{km}^{(0)}|f\rangle|^2 \, , \tag{1}$$

where

$$Q_{km}^{(0)} = \sum_{i=1}^{N} q_{km}^{(0)}(i) \, , \tag{2}$$

* National Academy of Sciences visiting research associate.

† Present address: Department of Physics, University of Windsor, Windsor, Ontario.

$$q_{km}^{(0)}(i) = \left(\frac{4\pi}{2k+1}\right)^{1/2} [\nabla r_i^k Y_k^m(\theta_i,\phi_i)]\left[\frac{l_i}{k+1} + s_i\right] , \quad (3)$$

ω is the transition frequency, and $c = 1/\alpha$ (Akhiezer and Berestetskii 1965). Equation (3) may be written in terms of irreducible tensor operators by use of the relation

$$\nabla r^k Y_k^m(\theta_i,\phi_i) = [k(2k+1)]^{1/2} r^{k-1} \mathbf{Y}_{k,k-1,m_k} ,$$

where $\mathbf{Y}_{klm}$ is a vector spherical harmonic. In the notation of Edmonds (1960), the result for LS-coupled states is

$$\begin{aligned}\langle\gamma' L'S'M' | q_{km}^{(0)}(i) | \gamma LSJM\rangle \\ &= (-1)^{J'-M'} \begin{pmatrix} J' & k & J \\ -M' & m & M \end{pmatrix} (\gamma' L'S'J' \| q_k^{(0)}(i) \| \gamma LSJ)\end{aligned} \quad (4)$$

and

$$\begin{aligned}&\gamma' L'S'J' \| q_k^{(0)}(i) \| \gamma LSJ) \\ &= (4\pi k)^{1/2} \Big[\frac{\delta_{s,s'}}{k+1} (2k+1)^{1/2} (-1)^{k+L+L'} \sum_{\gamma'' L''} \begin{Bmatrix} k-1 & 1 & k \\ L & L' & L'' \end{Bmatrix} \\ &\quad \times (\gamma' L' \| r_i^{k-1} Y_{k-1}(i) \| \gamma'' L'')(\gamma'' L'' \| l_i \| \gamma L) \\ &\quad + [(2J+1)(2J'+1)(2k+1)]^{1/2} \begin{Bmatrix} L' & L & k-1 \\ S' & S & 1 \\ J' & J & k \end{Bmatrix} \\ &\quad \times \sum_{\gamma''} (\gamma' L' \| r_i^{k-1} Y_{k-1}(i) \| \gamma'' L'')(\gamma'' S' \| s_i \| \gamma S) \Big] .\end{aligned} \quad (5)$$

For the ${}^3P_{J'}$–${}^1S_0$ magnetic-quadrupole transition, the first term of equation (5) makes no contribution and the second vanishes unless $J' = 2$ due to the 9-j symbol-selection rules. For $J' = 2$, equation (5) reduces to

$$({}^3P_2 \| q_k^{(0)}(i) \| {}^1S_0) = \tfrac{2}{3}(10\pi)^{1/2} ({}^3P \| r_i Y_1(i) \| {}^1S)({}^3P \| s_i \| {}^1S) . \quad (6)$$

For a two-electron atom,

$$({}^3P \| s_1 \| {}^1S) = -({}^3P \| s_2 \| {}^1S) = \tfrac{1}{2}\sqrt{3} ,$$

and the matrix element of $Q_{2m}^{(0)}$ may be written in terms of the z-component of the transition as

$$\langle i | Q_{2m}^{(0)} | f \rangle = (\sqrt{3}/\sqrt{2}) \langle {}^3P | z_1 - z_2 | {}^1S \rangle . \quad (7)$$

The symbols ${}^3P$ and ${}^1S$ denote, respectively, the antisymmetric and symmetric uncoupled spatial portions of the normalized eigenfunctions. Equation (7) agrees with the work of Garstang (1967). The decay rate from equation (1) is, in atomic units,

$$A_{2m}^{(0)} = \frac{1}{10c^2}\left(\frac{\omega}{c}\right)^5 | \langle {}^3P | z_1 - z_2 | {}^1S \rangle |^2 . \quad (8)$$

III. VARIATIONAL CALCULATIONS

The 2^3P and 1^3S eigenfunctions were represented by correlated variational functions of the form

$$\psi^{LSM_L} = \frac{1}{\sqrt{2}}(1 \pm P_{12}) \sum_{ijk} a_{ijk}{}^{LS} \phi_{ijk}{}^{LS}(r_1,r_2)\, Y_{Ll_1l_2}{}^{M_L}(\Omega_1,\Omega_2) \; ,$$

$$Y_{Ll_1l_2}{}^{M_L}(\Omega_1,\Omega_2) = \sum_{m_1m_2} \langle l_1m_1l_2m_2 | LM_L \rangle Y_{l_1}{}^{m_1}(\Omega_1)\, Y_{l_2}{}^{m_2}(\Omega_2) \; , \tag{9}$$

$$\phi_{ijk}{}^{LS}(r_1,r_2) = r_1{}^i r_2{}^j r_{12}{}^k \exp\,(-\,\alpha^{LS} r_1 - \beta^{LS} r_2) \; ,$$

and P_{12} indicates the interchange of 1 and 2. The plus sign refers to singlet states and the minus sign to triplet states. The linear parameters $a_{ijk}{}^{LS}$ were determined by solution of the secular problem, and the scale factors α^{LS} and β^{LS} were chosen by optimization of the 2^3P and 1^1S energies. Fifty terms were retained in the wave functions for $Z = 2$ and 3, and thirty terms for $Z = 4$–10.

TABLE 1

2^3P_2–1^1S_0 MAGNETIC-QUADRUPOLE DECAY RATES $A_{2m}{}^{(0)}$ (sec^{-1})

System	Z-Expansion	Variational	Garstang (1967)	Mizushima (1966)
He I	4.00×10^{-1}	3.27×10^{-1}	2.2×10^{-1}	1.5
Li II	3.60×10^{1}	3.50×10^{1}	...	10^2
Be III	6.14×10^{2}	6.17×10^{2}	...	10^3
B IV	4.97×10^{3}	5.01×10^{3}		5×10^3
C V	2.58×10^{4}	2.62×10^{4}	...	5×10^4
N VI	1.01×10^{5}	1.03×10^{5}		10^5
O VII	3.26×10^{5}	3.31×10^{5}	3.0×10^{5}	5×10^5
F VIII	9.02×10^{5}	9.16×10^{5}	...	10^6
Ne IX	2.23×10^{6}	2.26×10^{6}	...	
Na X	5.06×10^{6}			
Mg XI	1.06×10^{7}			
Al XII	2.08×10^{7}			
Si XIII	3.87×10^{7}			
P XIV	6.92×10^{7}			
S XV	1.19×10^{8}			
Cl XVI	1.97×10^{8}			
A XVII	3.18×10^{8}			

The decay rates obtained from equation (8) are given in Table 1. Theoretically calculated nonrelativistic energy differences were used in the calculation of the decay rates. Agreement is within the accuracy of Garstang's (1967) results and also Mizushima's (1966) results for larger values of the nuclear charge.

IV. Z-EXPANSION CALCULATIONS

Suppose $\phi_s{}^{(0)}$ is some approximate representation of the eigenfunction ψ_s of the sth state of an atomic system and $E_s{}^{(0)}$ an approximation to the eigenvalues E_s such that

$$H\psi_s = E_s\psi_s \tag{10}$$

and

$$H_s\psi_s{}^{(0)} = E_s{}^{(0)}\psi_s{}^{(0)} \; , \tag{11}$$

with equation (11) defining the effective Hamiltonian H_s. Cohen and Dalgarno (1966) have shown that, if L is any function of the electronic coordinates, the right-hand side of

$$\langle\psi_s|L|\psi_t\rangle = \langle\phi_s{}^{(0)}|L|\phi_t{}^{(0)}\rangle + \langle\chi_s|H|\phi_s{}^{(0)}\rangle + \langle\chi_t|H|\phi_t{}^{(0)}\rangle \tag{12}$$

is stationary with respect to first-order variations of $\phi_s^{(0)}$ and $\phi_t^{(0)}$. Here

$$(H_s - E_s^{(0)})\chi_s + L\phi_t^{(0)} - \langle\phi_t^{(0)}|L|\phi_s^{(0)}\rangle\phi_s^{(0)} = [\langle\phi_t^{(0)}|H_s - E_s^{(0)}|\chi_s\rangle + \langle\phi_t^{(0)}|L|\phi_t^{(0)}\rangle]\phi_t^{(0)} \tag{13}$$

such that

$$\langle\chi_s|\phi_s^{(0)}\rangle = \langle\phi_s^{(0)}|\phi_t^{(0)}\rangle = 0\,. \tag{14}$$

It is customary to redefine the units of energy and length to be Z^2 and $1/Z$ atomic units, respectively. Then, if H_s and H_t are defined by

$$H_s = H_t = \sum_{i=1}^{N} - \tfrac{1}{2}\nabla_i^2 - 1/r_i$$

and L is a sum of one-electron operators, equation (13) splits into a sum of one-electron equations which may be solved exactly.

Dalgarno and Parkinson (1967) have solved equation (13) for $1s^2\ {}^1S$–$1s\ np\ {}^1P$ electric-dipole transitions for which $L = z_1 + z_2$. For $1s^2\ {}^1S$–$1s\ np\ {}^3P$ magnetic-quadrupole transitions, $L = z_1 - z_2$ and equation (13) splits into exactly the same one-electron equations as for the electric-dipole case. Dalgarno and Parkinson write the Z-expansion of the electric-dipole transition integral in the form

$$\langle{}^1S|z_1 + z_2|n{}^1P\rangle = (2^{1/2}/Z)\{A(n) + Z^{-1}[I_1(n) + I_2(n) + I_3(n) + I_4(n)]\}\,. \tag{15}$$

The corresponding Z-expansion of the magnetic-quadrupole transition is then

$$\langle{}^1S|z_1 - z_2|n{}^3P\rangle = (2^{1/2}/Z)\{A(n) + Z^{-1}[I_1(n) + I_2(n) - I_3(n) + I_4(n)]\}\,. \tag{16}$$

The $A(n)$ and $I_i(n)$ are tabulated by Dalgarno and Parkinson for $n = 2(1)\ 20$. The Z-expansion of the Hartree-Fock approximation is obtained by omitting $I_4(n)$ in equations (15) and (16), since this term corresponds to virtual excitations of the passive $1s$ electron (see Dalgarno and Parkinson [1967] for further details).

If we adopt the screening approximation of Dalgarno and Stewart (1960), the expression corresponding to equation (7) for the magnetic-quadrupole transition integral is

$$\langle n{}^3P|z_1 - z_2|1\,{}^1S\rangle = \frac{2^{1/2}A(n)}{Z - \sigma(n)}\,, \tag{17}$$

where $\sigma(n) = [I_1(n) + I_2(n) - I_3(n) + I_4(n)]/A(n)$ and the Hartree-Fock transition integral is given by

$$\langle n{}^3P|z_1 - z_2|1\,{}^1S\rangle_{\mathrm{HF}} = \frac{2^{1/2}A(n)}{Z - \sigma_{\mathrm{HF}}(n)}\,, \tag{18}$$

where $\sigma_{\mathrm{HF}}(n) = \sigma(n) - I_4(n)/A(n)$. Values of $A(n)$, $\sigma(n)$, and $\sigma_{\mathrm{HF}}(n)$ are given in Table 2. The 2^3P–1^1S decay rates obtained from equation (17) are compared with the variational results in Table 1. The magnetic-quadrupole Z-expansion converges to the variational results much more rapidly than does the electric-dipole expansion obtained by Dalgarno and Parkinson. Equation (17) thus provides a reliable method of extrapolating the variational results. One may also expect smaller errors in equation (17) with increasing n than those occurring in the electric-dipole expansion. The latter overestimates the electric-dipole oscillator strengths by 35 percent at $Z = 2$ and $n = 2$, and the error tends to a limiting value of 72 percent as n increases.

V. DISCUSSION

The 2^3P_2–1^1S_0 magnetic-quadrupole decay rate increases asymptotically along the isoelectronic sequence as Z^8, while the competing 2^3P_2–2^3S_1 electric-dipole rate increases only as Z. Thus, the magnetic-quadrupole rate reaches 10 percent of the electric-dipole rate at Mg XI (see Table 1) and becomes the dominant 2^3P_2 radiative-decay process for the ions beyond Cl XVI.

The leading term in the 2^3P_1–1^1S_0 spin-orbit electric-dipole decay rate is also proportional to Z^8, provided Z is not greater than about 20. For Z less than 20, the rates are

TABLE 2

VALUES OF $A(n)$, $\sigma(n)$, AND $\sigma_{HF}(n)$

n	$A(n)$	$\sigma(n)$	$\sigma_{HF}(n)$
2	7.4494×10^{-1}	0.1466	0.1959
3	2.9831×10^{-1}	.2697	.3292
4	1.7585×10^{-1}	.3066	.3695
5	1.2050×10^{-1}	.3210	.3855
6	8.9567×10^{-2}	.3274	.3927
7	7.0102×10^{-2}	.3304	.3962
8	5.6868×10^{-2}	.3318	.3979
9	4.7369×10^{-2}	.3323	.3987
10	4.0269×10^{-2}	.3324	.3989
11	3.4793×10^{-2}	.3323	.3989
12	3.0461×10^{-2}	.3319	.3986
13	2.6964×10^{-2}	.3316	.3984
14	2.4091×10^{-2}	.3313	.3982
15	2.1696×10^{-2}	.3309	.3978
16	1.9675×10^{-2}	.3305	.3971
17	1.7950×10^{-2}	.3301	.3974
18	1.6464×10^{-2}	.3297	.3967
19	1.5172×10^{-2}	.3293	.3963
20	1.4042×10^{-2}	0.3290	0.3960

uniformly about 3 orders of magnitude faster than the magnetic-quadrupole rates given in Table 1. For larger values of Z, the singlet-triplet mixing becomes saturated and the spin-orbit electric-dipole process increases only as Z^4. However, the calculation is further complicated by the need for explicit relativistic corrections to the wave functions and energies.

This work has been partly supported by NASA grant NGR22-007-136.

REFERENCES

Akhiezer, A. I., and Berestetskii, V. B. 1965, *Quantum Electrodynamics* (New York: Interscience Publishers).
Cohen, M., and Dalgarno, A. 1966, *Proc. Roy. Soc. London, A*, **293**, 359.
Dalgarno, A., and Parkinson, E. M. 1967, *Proc. Roy. Soc. London, A*, **301**, 253.
Dalgarno, A., and Stewart, A. L. 1966, *Proc. Roy. Soc. London, A*, **257**, 534
Drake, G. W. F., and Dalgarno, A. 1969, *Ap. J.*, **157**, 459.
Edmonds, A. R. 1960, *Angular Momentum in Quantum Mechanics* (Princeton, N.J.: Princeton University Press).
Evans, K., and Pounds, K. A. 1968, *Ap. J.*, **152**, 319.
Garstang, R. H. 1967, *Ap. J.*, **148**, 579.
Meekins, J. F., Kreplin, R. W., Chubb, J. A., and Friedman, H. 1968, *Science*, **162**, 891.
Mizushima, M. 1964, *Phys. Rev.*, **134**, A883.
———. 1966, *J. Phys. Soc. Japan*, **21**, 2335.
Neupert, W. M , Gates, W., Swartz, M., and Young, R. 1967, *Ap. J. (Letters)*, **149**, L79.
Widing, K. G., and Sandlin, G. D. 1968, *Ap. J.*, **152**, 545.

PHYSICAL REVIEW A VOLUME 3, NUMBER 3 MARCH 1971

Theory of Relativistic Magnetic Dipole Transitions: Lifetime of the Metastable 2 ^3S State of the Heliumlike Ions

G. W. F. Drake
Department of Physics, University of Windsor, Windsor, Ontario, Canada
(Received 16 September 1970)

It has recently been established that the radiative lifetime of the metastable 2 ^3S state of helium and the heliumlike ions is determined by single-photon magnetic dipole ($M1$) transitions to the ground state, rather than the two-photon process proposed by Breit and Teller. The theory of $nl-n'l$ $M1$ transitions with $n \neq n'$ is developed in the Pauli approximation and extended to two-electron systems. Terms arising from relativistic energy corrections and finite-wavelength effects are included. The results for hydrogenic systems are shown to be identical to those obtained in the relativistic four-component Dirac formulation. The coefficients in the Z^{-1} perturbation expansion of the $1s2s\,^3S$–$1s^2\,^1S$ $M1$ transition integral are evaluated through ninth order and used to calculate the $M1$ emission probabilities from the 2 ^3S state of the two-electron ions up to Fe xxv. The emission probability for neutral helium is 1.27×10^{-4} sec^{-1}. The results are compared with recent solar coronal observations by Gabriel and Jordan, and with a measurement of the 2 ^3S state lifetime in Ar xvii by Schmieder and Marrus.

The $M=0$ component of the magnetic dipole transition matrix element then reduces to

$$\langle 1\,^1S|Q_{10}|2\,^3S\rangle = \mu_B\langle 1\,^1S| -(2/3m^2c^2)(p_1^2-p_2^2) - \tfrac{1}{6}(\omega/c)^2(r_1^2-r_2^2) + (Ze^2/3mc^2)(r_1^{-1}-r_2^{-1})|2\,^3S\rangle, \tag{35}$$

omitting the spin parts of the wave functions. The

TABLE II. $1s2s\ ^3S$-$1s^2\ ^1S$ energy differences, transition integrals,[a] and $M1$ decay rates for the heliumlike ions.

Z	ΔE(a.u.)[b]	p^2/Z^2	Z^2r^2	$1/(Zr)$	A_{i-f}(sec^{-1})
2	0.72850	0.43844	−7.4984	0.27412	1.272×10^{-4}
3	2.16918	0.49290	−6.0779	0.28532	2.039×10^{-2}
4	4.35840	0.51837	−5.5126	0.28903	5.618×10^{-1}
5	7.29707	0.53337	−5.2099	0.29087	6.695×10^{0}
6	10.98549	0.54330	−5.0215	0.29197	4.856×10^{1}
7	15.42376	0.55036	−4.8929	0.29269	2.532×10^{2}
8	20.61194	0.55565	−4.7997	0.29321	1.044×10^{3}
9	26.55007	0.55976	−4.7289	0.29360	3.608×10^{3}
10	33.23815	0.56305	−4.6734	0.29390	1.087×10^{4}
11	40.67621	0.56574	−4.6287	0.29414	2.935×10^{4}
12	48.86425	0.56797	−4.5920	0.29434	7.243×10^{4}
13	57.80226	0.56987	−4.5612	0.29450	1.658×10^{5}
14	67.49027	0.57149	−4.5350	0.29464	3.563×10^{5}
15	77.92826	0.57290	−4.5125	0.29476	7.251×10^{5}
16	89.11625	0.57413	−4.4930	0.29486	1.408×10^{6}
17	101.0542	0.57521	−4.4758	0.29495	2.622×10^{6}
18	113.7422	0.57618	−4.4607	0.29503	4.709×10^{6}
19	127.1802	0.57704	−4.4472	0.29510	8.187×10^{6}
20	141.3681	0.57782	−4.4351	0.29516	1.383×10^{7}
21	156.3061	0.57852	−4.4242	0.29522	2.275×10^{7}
22	171.9941	0.57916	−4.4143	0.29527	3.656×10^{7}
23	188.4320	0.57975	−4.4053	0.29532	5.751×10^{7}
24	205.6200	0.58028	−4.3971	0.29536	8.870×10^{7}
25	223.5579	0.58077	−4.3895	0.29540	1.344×10^{8}
26	242.2459	0.58123	−4.3826	0.29544	2.002×10^{8}

[a] An operator $\mathcal{O}$ is understood to mean $\mathcal{O}_1 - \mathcal{O}_2$, with the spin parts of the wave functions omitted when calculating matrix elements. Atomic units are used except as noted.

[b] Nonrelativistic energy differences are used throughout. Relativistic corrections increase the A_{i-f} values by less than 1 or 2% for $Z \lesssim 20$.

Radiative Decay of the 2^3S_1 and 2^3P_2 States of Heliumlike Vanadium ($Z = 23$) and Iron ($Z = 26$)*

Harvey Gould, Richard Marrus,† and Peter J. Mohr
Department of Physics and Lawrence Berkeley Laboratory, University of California, Berkeley, California 94720
(Received 1 July 1974)

Lifetimes of the $M1$ decay $2^3S_1 \to 1^1S_0$ and of the decay $2^3P_2 \to 1^1S_0$ have been measured in the two-electron ions V^{+21} and Fe^{+24}. The measured lifetimes are $\tau(2^3S_1) = 16.9(7)$ nsec for V^{+21} and $\tau(2^3S_1) = 4.8(6)$ nsec for Fe^{+24}. The 2^3P_2 lifetimes are compared with a calculation that considers relativistic corrections and hyperfine-structure effects. It is found that for V^{+21}, hyperfine effects contribute appreciably to the lifetime. For Fe^{+24} we obtain $\tau(2^3P_2) = 0.11(2)$ nsec.

TABLE I. Theoretical transition rates and lifetimes of the 2^3P_2 state in heliumlike ions.

Z	A_{E1} (nsec^{-1})	A_{M2} (nsec^{-1})	F	$A_{E1}{}^{\mathrm{hfs}}$ (nsec^{-1})	τ (nsec)
16	0.259	0.117			2.66
17	0.301	0.194	All	< 0.007	$\simeq$ 2.01
18	0.352	0.312			1.51
22	0.687	1.64			0.429
23	0.820	2.37	3/2	0	0.313
			5/2	0.99	0.239
			7/2	1.75	0.202
			9/2	1.69	0.205
			11/2	0	0.313
26	1.43	6.50			0.126

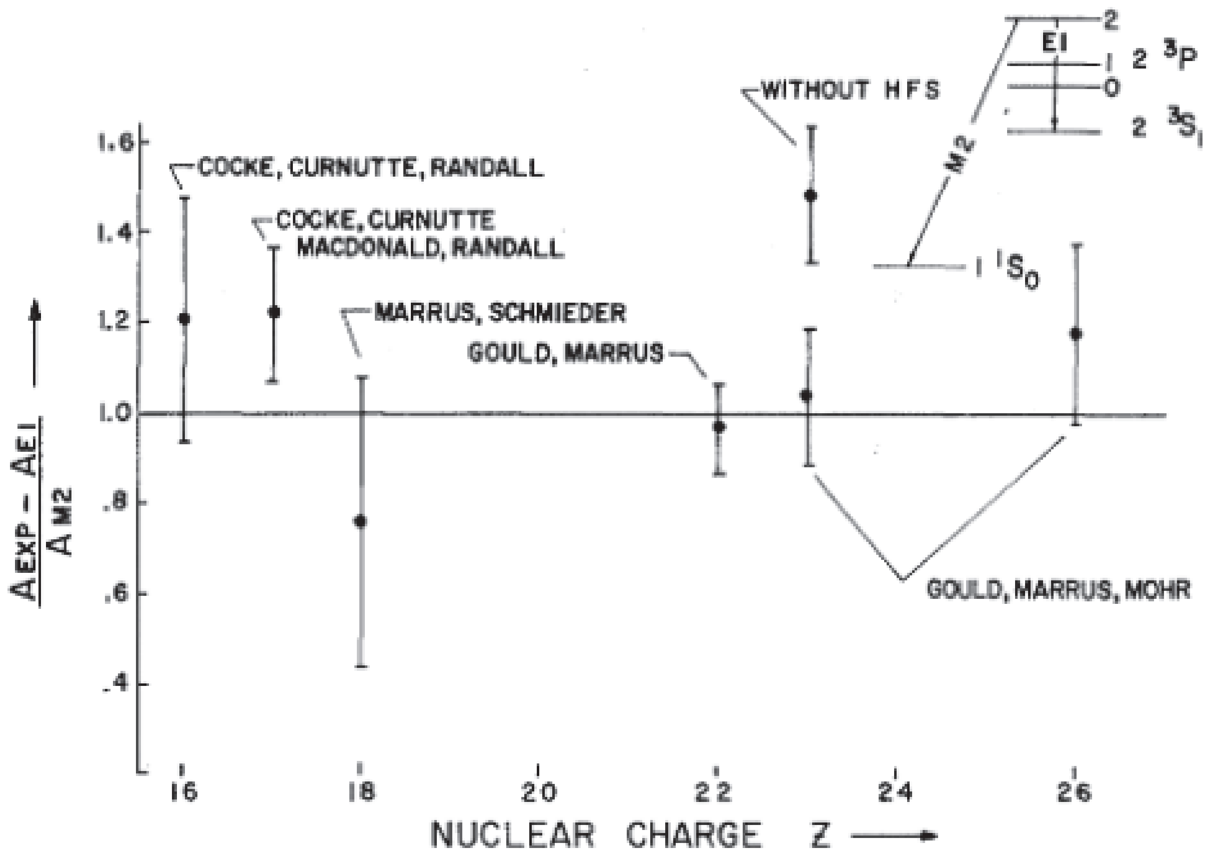

FIG. 3. Comparison between measured and calculated $M2$ rates for decay from the 2^3P_2 level. The point at $Z = 23$ labeled "without HFS" is obtained by making a best fit to our vanadium data using a single exponential.

PHYSICAL REVIEW A VOLUME 12, NUMBER 6 DECEMBER 1975

Experimental determination of the single-photon transition rate between the $2\,^3S_1$ and $1\,^1S_0$ states of He I †

Joseph R. Woodworth*‡ and H. Warren Moos
Department of Physics, The Johns Hopkins University, Baltimore, Maryland 21218
(Received 7 July 1975)

The highly forbidden single-photon transition rate between the $2\,^3S_1$ and $1\,^1S_0$ states of He I has been measured in a radio-frequency He discharge. The population of metastables in the $2\,^3S_1$ state was determined by Fabry-Perot interferometric profiles of absorption from the $2\,^3S_1$ to the $4\,^3P_{0,1,2}$ states. High spectral resolution and precision ultraviolet radiometry were used to determine the brightness of the emission feature observed at 625.54 ± 0.05 Å, compared to the theoretical value of 625.56 Å. Because of the very low transition rate, this feature is weak, but it is shown that it is due to the $2\,^3S_1$-$1\,^1S_0$ transition. The value for the radiative transition
rate obtained in t ... omparison to the
theoretical value ... iments which
have measured th

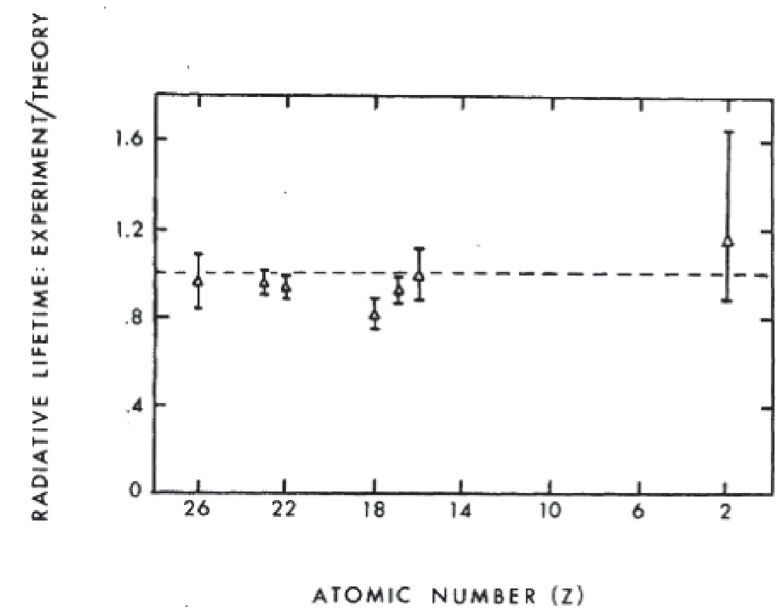

FIG. 5. Comparison of experimental and theoretical $2\,^3S_1$ lifetimes for various values of Z.

Hyperfine quenching of the $2^3P_{0,2}$ states in He-like ions

A.V. Volotka, V.M. Shabaev, G. Plunien, G. Soff, and V.A. Yerokhin

Abstract: The transition probabilities of the lines $1^1S_0 - 2^3P_0$ and $1^1S_0 - 2^3P_2$ in He-like ions with nonzero nuclear spins are calculated. The hyperfine-quenching effect on the lifetimes of the $2^3P_{0,2}$ states is investigated. The Coulomb and Breit interelectronic interactions are taken into account to the order $(\alpha Z)^2/Z$ by means of perturbation theory. The calculation is performed for both length and velocity gauges. The transition rates evaluated are in good agreement with previous $1/Z$ and CI calculations.

Can. J. Phys. **80**: 1263–1269 (2002)

Table 1. The lifetimes of the 2^3P_0 state of He-like ions with nonzero nuclear spins in the range $Z = 15$–30. The transition probabilities Ω_{E1} corresponding to the line $2^3S_1 - 2^3P_0$ are taken from ref. 4. In columns 5–8, the transition probabilities of the hyperfine-induced decay are presented. $\Omega_\mu^{l,v}$ are the results of this work obtained within the length and velocity gauge, while $\Omega_\mu(1/Z)$ and $\Omega_\mu(CI)$ are taken from refs. 2 and 4, respectively. $\tau^{l,v}$ are the lifetimes of the 2^3P_0 state within the length and velocity gauge, also obtained in this work. For comparison, in the last two columns the lifetimes $\tau(CI)$ obtained by the relativistic CI calculation [4] and experimental lifetimes τ_{expt} are presented as well. The transition probabilities and the lifetimes are given in ns^{-1} and in ns, respectively. μ_I is the nuclear magnetic moment expressed in units of the nuclear magneton.

Ion	μ_I	I	Ω_{E1}	Ω_μ^l	Ω_μ^v	$\Omega_\mu(CI)$	$\Omega_\mu(1/Z)$	τ^l	τ^v	$\tau(CI)$	τ_{expt}
$^{31}P^{13+}$	1.1316	1/2	0.1659	0.0415	0.0411	0.0409	0.041	4.821	4.830	4.836	4.88(9)[a]
$^{33}S^{14+}$	0.64382	3/2	0.1799	0.0117	0.0116	0.0116		5.218	5.221	5.223	
$^{35}Cl^{15+}$	0.82187	3/2	0.1944	0.0302	0.0299	0.0297	0.030	4.453	4.458	4.462	
$^{36}Cl^{15+}$	1.28547	2	0.1944	0.0665	0.0660	0.0655		3.833	3.841	3.848	
$^{37}Cl^{15+}$	0.68412	3/2	0.1944	0.0209	0.0207	0.0206		4.645	4.648	4.652	
$^{39}K^{17+}$	0.39149	3/2	0.2250	0.0163	0.0162	0.0160	0.016	4.144	4.146	4.149	
$^{40}K^{17+}$	−1.2981	4	0.2250	0.1337	0.1328	0.1317		2.788	2.795	2.804	
$^{41}K^{17+}$	0.21488	3/2	0.2250	0.0049	0.0049	0.0048		4.350	4.350	4.351	
$^{41}Ca^{18+}$	−1.5948	7/2	0.2412	0.3144	0.3124	0.3095		1.800	1.806	1.816	
$^{43}Ca^{18+}$	−1.3176	7/2	0.2412	0.2148	0.2133	0.2114		2.193	2.200	2.209	
$^{45}Sc^{19+}$	4.7565	7/2	0.2581	4.2498	4.2235	4.181	4.15	0.2218	0.2231	0.2253	
$^{47}Ti^{20+}$	−0.78848	5/2	0.2758	0.1868	0.1857	0.1836		2.162	2.167	2.177	
$^{49}Ti^{20+}$	−1.1042	7/2	0.2758	0.3364	0.3345	0.3307		1.633	1.639	1.649	
$^{50}V^{21+}$	3.3457	6	0.2941	4.1568	4.1344	4.084		0.2247	0.2258	0.2284	
$^{51}V^{21+}$	5.1487	7/2	0.2941	10.918	10.859	10.73	10.5	0.0892	0.0897	0.09075	
$^{53}Cr^{22+}$	−0.47454	3/2	0.3134	0.1737	0.1728	0.1705		2.053	2.057	2.066	
$^{51}Mn^{23+}$	3.5683	5/2	0.3335	12.166	12.109	11.93		0.0800	0.0804	0.08154	
$^{55}Mn^{23+}$	3.4687	5/2	0.3335	11.493	11.439	11.27	10.7	0.0846	0.0849	0.08618	
$^{57}Fe^{24+}$	0.09062	1/2	0.3545	0.0241	0.0240	0.0236		2.641	2.642	2.645	
$^{59}Co^{25+}$	4.627	7/2	0.3765	39.182	39.028	38.32	36.0	0.0253	0.0254	0.02584	
$^{61}Ni^{26+}$	−0.75002	3/2	0.3996	1.8887	1.8819	1.845		0.4370	0.4383	0.4455	0.470(50)[b]
$^{63}Cu^{27+}$	2.2273	3/2	0.4239	24.425	24.345	23.80	21.7	0.0402	0.0404	0.04128	
$^{65}Cu^{27+}$	2.3816	3/2	0.4239	27.955	27.864	27.24		0.0352	0.0354	0.03615	
$^{67}Zn^{28+}$	0.8752	5/2	0.4493	4.4983	4.4851	4.373		0.2021	0.2027	0.2074	

[a]Livingston and Hinterlong [5] and Vogel-Vogt [6].
[b]Dunford et al. [7].

Table 2. The lifetimes of the 2^3P_2 state of He-like ions with nonzero nuclear spins in the range $Z = 15$–30. The transition probabilities $\Omega_{\rm E1}$ corresponding to the line $2^3S_1 - 2^3P_2$ are taken from ref. 19. $\Omega_{\rm M2}$ is the transition rate of the magnetic quadrupole decay $2^3P_2 \to 1^1S_0$ evaluated in this work. In columns 4–6, the transition probabilities of the hyperfine-induced decay are presented. $\Omega_\mu^{\rm l,v}$ are the results of this work in the length and velocity gauges, while Ω_μ(CI) is taken from ref. 4. $\tau^{\rm l,v}$ are the lifetimes of the 2^3P_2 state in the length and velocity gauges, obtained in this work. For comparison, in the last three columns the theoretical values of the lifetimes τ(CI) and $\tau(1/Z)$ from refs. 4 and 1 and the experimental lifetime $\tau_{\rm expt}$ for the case of $^{63}Cu^{27+}$, where the hyperfine-quenching effect contributes on the level of the current experimental accuracy, are presented. The transition probabilities and the lifetimes are given in ns^{-1} and in ns, respectively.

Ion	$\Omega_{\rm M2}$	$\Omega_{\rm E1}$	$\Omega_\mu^{\rm l}$	$\Omega_\mu^{\rm v}$	Ω_μ(CI)	$\tau^{\rm l}$	$\tau^{\rm v}$	τ(CI)	$\tau(1/Z)$	$\tau_{\rm expt}$
$^{31}P^{13+}$	0.0691	0.2214	0.0038	0.0037		3.398	3.399			
$^{33}S^{14+}$	0.1183	0.2562	0.0011	0.0011		2.662	2.662		2.66	
$^{35}Cl^{15+}$	0.1958	0.2978	0.0029	0.0029		2.014	2.014		2.01	
$^{36}Cl^{15+}$	0.1958	0.2978	0.0065	0.0064		2.000	2.000			
$^{37}Cl^{15+}$	0.1958	0.2978	0.0020	0.0020		2.018	2.018			
$^{39}K^{17+}$	0.4921	0.4079	0.0016	0.0016		1.109	1.109			
$^{40}K^{17+}$	0.4921	0.4079	0.0131	0.0130		1.095	1.095			
$^{41}K^{17+}$	0.4921	0.4079	0.0005	0.0005		1.111	1.111			
$^{41}Ca^{18+}$	0.7518	0.4809	0.0305	0.0303		0.7916	0.7918			
$^{43}Ca^{18+}$	0.7518	0.4809	0.0208	0.0207		0.7977	0.7978			
$^{45}Sc^{19+}$	1.1246	0.5697	0.3990	0.3960	0.3928	0.4777	0.4784	0.4795		
$^{47}Ti^{20+}$	1.6501	0.6782	0.0173	0.0171		0.4263	0.4264			
$^{49}Ti^{20+}$	1.6501	0.6782	0.0311	0.0308		0.4238	0.4239			
$^{50}V^{21+}$	2.3792	0.8109	0.3682	0.3656	0.3622	0.2810	0.2812	0.2817		
$^{51}V^{21+}$	2.3792	0.8109	0.9608	0.9541	0.9453	0.2409	0.2413	0.2420	0.253	
$^{53}Cr^{22+}$	3.3762	0.9735	0.0148	0.0147		0.2291	0.2291			
$^{51}Mn^{23+}$	4.7215	1.173	0.9753	0.9692	0.9584	0.1456	0.1457	0.1460		
$^{55}Mn^{23+}$	4.7215	1.173	0.9217	0.9158	0.9056	0.1467	0.1468	0.1471		
$^{57}Fe^{24+}$	6.5149	1.419	0.0018	0.0018		0.1260	0.1260		0.126	
$^{59}Co^{25+}$	8.8788	1.721	2.7853	2.7693	2.733	0.0747	0.0748	0.07504		
$^{61}Ni^{26+}$	11.962	2.092	0.1271	0.1264		0.0705	0.0705			
$^{63}Cu^{27+}$	15.946	2.549	1.4843	1.4765	1.453	0.0501	0.0501	0.05014		0.047(5)[a]
$^{65}Cu^{27+}$	15.946	2.549	1.6970	1.6881	1.662	0.0495	0.0495	0.04963		
$^{67}Zn^{28+}$	21.048	3.112	0.2531	0.2519		0.0410	0.0410			

[a]Buchet et al. [10].

Can. J. Phys. 99: 1–9 (2010)

Hyperfine Quenching: Review of Experiment and Theory

W.R. Johnson

Abstract: We give a brief outline of the theory of hyperfine quenching followed by a review of the progress that has been made in both theory and experiment since the pioneering work of Garstang [J. Opt. Soc. Am. **52**, 845 (1962)].

Radiation damping model in place of perturbation theory when level widths are Large compared with energy spacings

Lifetimes of silver isotopes (ns)

Ag^{107}	Rad. Damp.:	3.724	Expt:	3.97(37),
Ag^{109}	Rad. Damp.:	2.810	Expt:	2.84(32).